De novo neo-hyaline-cartilage from bovine organoids in viscoelastic hydrogels

Acta Biomaterialia 128 (2021) 236–249

Contents lists available at ScienceDirect

Acta Biomaterialia

journal homepage: www.elsevier.com/locate/actbio

Full length article

De novo neo-hyaline-cartilage from bovine organoids in viscoelastic hydrogels

João F. Crispim*, Keita Ito**

Orthopaedic Biomechanics group, Regenerative Engineering & Materials cluster, Dept. of Biomedical Engineering and the Institute for Complex Molecular Systems, Eindhoven University of Technology, The Netherlands

ARTICLE INFO

Article history:
Received 14 January 2021
Revised 31 March 2021
Accepted 1 April 2021
Available online 21 April 2021

Keywords:
Cartilage
Organoids
Viscoelastic hydrogel, Viscoelasticity,
Notochordal cell matrix

ABSTRACT

Regenerative therapies for articular cartilage are currently clinically available. However, they are associated with several drawbacks that require resolution. Optimizing chondrocyte expansion and their assembly, can reduce the time and costs of these therapies and more importantly increase their clinical success. In this study, cartilage organoids were quickly mass produced from bovine chondrocytes with a new suspension expansion protocol. This new approach led to massive cell proliferation, high viability and the self-assembly of organoids. These organoids were composed of collagen type II, type VI, glycosaminoglycans, with Sox9 positive cells, embedded in a pericellular and interterritorial matrix similarly to hyaline cartilage. With the goal of producing large scale tissues, we then encapsulated these organoids into alginate hydrogels with different viscoelastic properties. Elastic hydrogels constrained the growth and fusion of the organoids inhibiting the formation of a tissue. In contrast, viscoelastic hydrogels allowed the growth and fusion of the organoids into a homogenous tissue that was rich in collagen type II and glycosaminoglycans. The encapsulation of organoids to produce in vitro neocartilage also proved to be superior to the conventional method of encapsulating 2D expanded chondrocytes. This study describes a multimodal approach that involves chondrocyte expansion, organoid formation and their assembly into neohyaline-cartilage which proved to be superior to the current standard approaches used in cartilage tissue engineering.

Statement of significance

In this manuscript, we describe a new and simple methodology to quickly mass produce self-assembling cartilage organoids. Due to their matrix content and structure similarities with native cartilage, these organoids on their own have the potential to revolutionize cartilage research and the manner in which we study signaling pathways, disease progression, tissue engineering, drug development, etc. Furthermore, these organoids and their fast mass production were combined with a key relatively ignored hydrogel characteristic, viscoelasticity, to demonstrate their fusion into a neo-tissue. This has the potential to open the door for large scale cartilage regeneration such as for entire joint surfaces.

1. Introduction

One of the major challenges that societies in developed countries face today is their transition towards a much older population, which will lead to an increase in healthcare associated costs and a bigger burden for societies. Thus, osteoarthritis (OA) being the leading cause of disability and source of societal costs in older adults remains a challenge and a priority of the healthcare systems around the world [1]. The prevalence of OA is expected to continue increasing due to an aging population and according to the United Nations, by 2050 people aged over 60 years old will account for more than 20% of the world's population, and of those 20% it is estimated that 15% will have OA [2,3]. There are several therapies for the treatment of cartilage injuries such as microfracture,

* Corresponding author: João F. Crispim, Eindhoven University of Technology, Building 15, Gemini-South, Groene Loper, 5612 AZ Eindhoven, Netherlands.
** Co-corresponding Author: Keita Ito, Eindhoven University of Technology, Building 15, Gemini-South, Groene Loper, 5612 AZ Eindhoven, Netherlands.
E-mail addresses: j.f.ribeiro.pereira.simoes.crispim@tue.nl (J.F. Crispim), k.ito@tue.nl (K. Ito).

https://doi.org/10.1016/j.actbio.2021.04.008

abrasion arthroplasty and subchondral drilling that are designed to elicit a repair response with production of fibrocartilage [4,5]. Other techniques based on regenerative techniques such as autologous chondrocyte implantation (ACI) and matrix-assisted chondrocyte implantation (MACI) have also been explored for the treatment of full thickness cartilage lesions. Randomized control trials demonstrated clinical superiority of the MACI procedure when compared with other techniques such as microfracture [6,7]. However, there are many drawbacks of MACI and ACI. The neotissue may detach and/or inferior fibrocartilage may form [8,9]. It can take up to 21 months before the healing tissue fully matures with the right biomechanical properties [6,10]. It is expensive due to lengthy chondrocyte expansion [10]. Furthermore, the in vitro expansion of the chondrocytes is a delicate procedure as these cells will lose their chondrogenic phenotype and differentiate into fibroblast like cells leading to the formation of fibrocartilage [11–13]. There may be poor lateral integration between the neotissue and the surrounding native cartilage due to the low metabolic activity of the implanted chondrocytes [14]. Current chondrocyte expansion strategies rely on 2D systems, which is a slow process and is associated with the de-differentiation of chondrocytes, that can ultimately lead to the in vivo production of fibrocartilage. Hence, there is a need to develop strategies that can quickly expand chondrocytes without compromising their phenotype and synthetic capacity. Additionally, the long post-operative procedure can be shortened by implanting a more mature and metabolically active tissue that can integrate faster with the surrounding tissue. This would allow the patients to start with earlier and more aggressive rehabilitation, leading to a cost reduction and an improvement in patient's mobility and quality of life. In this study we developed a strategy to engineer neohyaline-cartilage in vitro which is based on a culture system to produce self-assembling cartilage organoids in large quantities and within a short period of time, and their fusion into neocartilage using viscoelastic hydrogels. To boost chondrocyte expansion while preserving their chondrogenic phenotype, we cultured bovine chondrocytes in a suspension culture, using spinner flasks, and notochordal cell derived matrix (NCM) as a supplement. NCM is a decellularized biologic matrix processed from porcine nucleus pulposus tissue, similar in composition to cartilage (rich in collagen type II and glycosaminoglycans, GAGs) and known to have a profound impact on chondrocytes and chondrocyte-like cells in terms of proliferation and matrix production [15–20]. We hypothesized that the chondrocytes would use the extracellular matrix (ECM) constituents from NCM and with time self-assemble into more complex structures resembling hyaline cartilage, i.e. organoids. We investigated the effect that NCM has on the proliferation, viability, organoid formation and its dimensions, composition and organization and then compared them with the standard expansion in 2D. These organoids were then encapsulated into different alginate hydrogels formulations with similar elasticity but different viscosity to study how viscoelasticity of the matrix affects cartilage formation by the organoids. Lastly, we compared our new approach with the conventional method of expanding chondrocytes in 2D followed by encapsulation, in terms of formation of in vitro neocartilage.

2. Material and methods

2.1. Production of porcine NCM

Nucleus pulposus tissue was harvested from the intervertebral disk of porcine donors (3 months old). Each batch of NCM consisted of NCM pooled from 3 independent donors. The harvested tissue was lyophilized (Labconco; Kansas City MO, USA) until it was completely dry. The product obtained consisted of a white and brittle matrix which was afterwards pulverized using a microdismembrator (Sartorius; Gottingen, Germany). The NCM powder was stored at −80 °C until further use.

2.2. Chondrocyte expansion

Cryovials were removed from the liquid nitrogen and placed in a 37 °C water bath until it started detaching from the walls of the cryovial. The frozen cells were resuspended in pre-warmed defrosting medium which consisted in hgDMEM containing 20% (v/v) FBS and 1% (v/v) (P/S). Next, the cells were centrifuged at 300 rcf for 5 min, the supernatant removed and the cells resuspended in defrosting medium and counted with a counting chamber. The cells were centrifuged again at 300 rcf for 5 min and resuspend at the concentration of 5×10^4 cells/mL in chondrocyte expansion medium with 0.25 mg/mL NCM or without NCM (negative control). Chondrocyte expansion medium consisted of 92% (v/v) hgDMEM, 5% (v/v) FBS, 1% (P/S), 1% (v/v) HEPES buffer (15,630,106, Gibco), 1% (v/v) non-essential amino acids (11,140,050, Gibco) and 0.2 mM L-Ascorbic acid 2-phosphate sesquimagnesium salt hydrate (A8960, Sigma-Aldrich). For the group cultured in medium with NCM, the NCM was first dissolved in hgDMEM with a homogenizer Ultra-Turrax (IKA; Staufen, Germany) until it was completely solubilized and then the other medium components were added. The working volume per spinner flask was 125 mL. The spinner flaks were placed on top of magnetic stirrer plate Variomag Biosytem 4 (Thermo Fischer Scientific; Waltham MA, USA) and the agitation set to 60 rpm with the help of a Biomodul 40B (Thermo Fischer Scientific). The entire setup was inside an incubator at 37 °C, 5% CO_2 and 2.5% O_2. Cells were cultured for 12 days inside the spinner flasks with medium refreshment at day 4, 8 and 11. At day 4, half of the medium (62.5 mL) was carefully removed from the flasks and centrifuged at 300 rcf for 10 min. Then the supernatant was removed, the pellet resuspended in fresh chondrocyte expansion medium with or without 1 mg/mL NCM, and added back to the respective spinner flask. On day 8 and 11, the total medium in the flask was refreshed and not just half of it like in day 4. Cells were not passaged in 2D before being used in the spinner flasks. For culturing chondrocytes in 2D, the cryovials were thawed as described above and the cells plated at the density of 15,000 cells/cm^2 in T500 flasks (132,913, Thermo Fischer Scientific) in chondrocyte expansion medium, with 10% FBS instead of 5%, and cultured until 80% confluent. Cells were used at passage 1 for gene expression studies and encapsulation in hydrogels as single cells.

2.3. Organoid analysis

At day 3, 6, 9 and 12, medium from the spinner flasks was collected to determine cell concentration, viability and organoid dimensions. Organoid dimensions were determined by pipetting 500 µL of the collected medium to a petri dish and imaged with an EVOS XL Core microscope (AMEX1000, Life Technologies; Carlsbad CA, USA). Pictures were processed with ImageJ software and the maximum and minimum Feret diameter of every organoid (Fig. A.1) determined. The root mean square between the maximum and minimum Feret diameter was calculated (Equation A.1) and used to determine the volume of an organoid by assuming they were a perfect sphere (Equation A.2). The cell concentration and viability inside the flask (with and without NCM) was determined by centrifuging, at 300 rcf for 10 min, the medium collected at every time point. Next, the supernatant was removed, the pellet resuspended in a digestion buffer, which consisted in hgDMEM with 0.1 mg/mL hyaluronidase and 2 mg/mL collagenase A (Roche), and incubated overnight at 37 °C and 5% CO_2 in a tube roller. Next day, the cell suspension was centrifuged at 300 rcf for 10 min, the supernatant removed and the pellet resuspend in hgDMEM. The cells suspension was mixed (1:1) with 0.4% (w/v) Trypan blue (15,250,061,

Gibco) and the cells counted using a counting chamber. Cell concentration was calculated by dividing the number of viable cells (cells not stained blue) by the total volume inside the spinner flask, and cell viability by dividing the number of viable cells by the total number of cells (not stained and blue stained cells).

2.4. Alginate fabrication and characterization

Alginic acid (71,238, Sigma-Aldrich) was reacted with different concentrations of H_2O_2 (216,763, Sigma-Aldrich) at different temperatures to obtain alginate with different average molecular weights. First, a 2% (w/v) solution of the standard alginate (average molecular weight of 298 kDa) was prepared in milliQwater and warmed to the desire temperature with the help of a hot plate, a heating jacket and an electronic contact thermometer (VT-5, VWR). Once the alginate solution reached the desired temperature, H_2O_2 was added, and the reaction carried out for 2 h with an agitation of 600 rpm. To fabricate alginate with an average molecular weight of 170 kDa, the reaction was carried at 60 °C with 0.25% (v/v) H_2O_2, the 70 kDa alginate was obtained carrying the reaction at 85 °C with 0.25% (v/v) H_2O_2 and the 48 kDa alginate at 85 °C with 1.5% (v/v) H_2O_2. After 2 h, the reaction was stopped by freezing the solutions at −30 °C overnight. Next day, the samples were thawed and purified with a 3.5 kDa molecular weight cut off dialysis cassette (66,110, Thermo Fischer Scientific) in milliQwater for 48 h. The water was replaced after 2, 4 and 24 h. After dialysis, the samples were collected from the cassettes to tubes and frozen at −80 °C overnight. Next day the samples were lyophilized until they were completely dried. The 298 kDa alginate was not reacted with H_2O_2, but it was purified by dialysis and lyophilized like the other alginates. The lyophilized samples were stored at room temperature until further used. The molecular weight of the alginates was assessed by gel permeability chromatography (GPC).

2.5. Hydrogel fabrication and characterization

A 2.5% (w/v) solution of alginate was prepared in hgDMEM and added to a 3 mL syringe. Next, a solution of $CaSO_4$ (102,161, Supelco; St Louis MO, USA) was prepared in hgDMEM and added to a second 3 mL syringe. Depending on the molecular weight, the alginate was crosslinked with different concentrations of $CaSO_4$. The 298 kDa alginate was crosslinked with 125 mM $CaSO_4$, the 170 kDa with 166.5 mM $CaSO_4$, the 70 kDa with 212.5 mM $CaSO_4$ and the 48 kDa with 275 mM $CaSO_4$. The ratio inside the syringes between the volume of the alginate solution and the volume of the $CaSO_4$ solution was 4:1. The two syringes were connected with a female-female Luer lock coupler system (21,015, Supelco) and then the two solutions (alginate and $CaSO_4$) were mixed. The mixture was deposited on a Teflon mold, with wells of 8 mm diameter and 2 mm height. Next, a glass slide was placed on top of the mold, the glass and mold clamped together with paper clips, and then the solution was allowed to gel for 45 min. After 45 min, the hydrogels were placed inside a well plate and allowed to swell overnight in chondrocyte experiment medium containing 1 mM $CaCl_2$ before characterization. Chondrocyte experiment medium was identical to the chondrocyte expansion medium described above, but with 10% FBS instead of 5%. Mechanical characterization of the hydrogels was performed in an ARES rheometer (TA Instruments; Asse, Belgium). Hydrogels were placed in the pre-warmed (37 °C) lower plate of the rheometer and the top plate lowered until a force of 0.05 N was applied to ensure contact between the hydrogel and the top plate. A plate with a parallel geometry and 8 mm diameter was used. PBS containing 1 mM $CaCl_2$ was applied to the hydrogel to prevent evaporation and the hydrogel allowed to equilibrate to 37 °C for 10 min. After 10 min, a dynamic time sweep test was performed for 300 s, at a frequency of 1 Hz and strain of 1% at 37 °C. All hydrogels were then subjected to a dynamic strain sweep test, from 0.1 to 100% strain, at the frequency of 1 Hz and 37 °C, to confirm that 1% strain was within the linear behavior of the hydrogel. For swelling and degradation studies, the hydrogels were incubated in chondrocyte experiment medium containing 1 mM $CaCl_2$ at 37 °C, 5% CO_2 and 2.5% O_2, and their weight measured after 1 and 24 days. First their wet weight was measured and then the hydrogels were frozen at −80 °C overnight. Next day, the hydrogels were lyophilized overnight and afterwards their dry weight was measured. The swelling ratio was calculated as the ratio between the wet and the dry weight.

2.6. Organoid and cell encapsulation in the hydrogels

After 12 days of culture inside the spinner flaks, the organoids were collected and strained through a 100 µm cell strainer, followed by 3 times washing with PBS. Next, the strained organoids were mixed with the 2.5% (w/v) alginate solution and the hydrogels fabricated as described above. The organoids were seeded into the hydrogels at the volumetric concentration (v/v) of 50% organoids/hydrogel. The median volume of the organoids, after 12 days of culture inside the spinner flasks, was used to calculate the amount of organoids needed to be encapsulated. The hydrogels containing organoids were then cultured for 24 days in chondrocyte experiment medium containing 1 mM $CaCl_2$ at 37 °C, 5% CO_2 and 2.5% O_2. Medium was refreshed three times a week.

Cells cultured in 2D (Passage 1) were trypsinized with 0.05% trypsin-EDTA (25,300–054, Gibco) before confluency, counted with a counting chamber and mixed with 2.5% (w/v) 48 kDa alginate at the concentration of 110.000.000 cells/mL. This concentration was chosen, so that the number of cells per hydrogel matched the number of cells in the hydrogels with organoids. The amount of DNA measured on day 1 for the hydrogels with organoids was used as a reference to calculate the amount of single cells needed, assuming that each cell contains 6 pg of DNA. Hydrogels with single cells were fabricated and cultured as described above.

To study the stability of tissue constructs after 24 days of culture, alginate hydrogels were disassociated by incubating them with sodium citrate buffer for one hour with gentle shaking at room temperature.

2.7. Statistical analysis

All experiments were conducted with at least three replicates per group. Proliferation and viability studies inside the spinner flask were conducted with three donors. To compare organoid volume, the data population ($n > 100$) was checked for normality using D'Agostino & Pearson normality test (did not follow normal distribution) and then compared using a one-tailed nonparametric Mann Whitney *t*-test. One-way ANOVA with post hoc Bonferroni's multiple comparison test was used to test for significance between groups within the same time point, while two-way ANOVA was used to test for significance within groups across multiple time points. Comparisons with $p < 0.05$ were considered statistically significant. All statistical tests were performed using GraphPad Software.

3. Results

3.1. Fast production of organoids in large quantities

Bovine chondrocytes were cultured in spinner flasks for 12 days with or without solubilized NCM, and the proliferation, viability and organoid volume and composition were analyzed at different time points. In terms of proliferation, chondrocytes cultured with NCM proliferated much faster than the negative control (Fig. 1a).

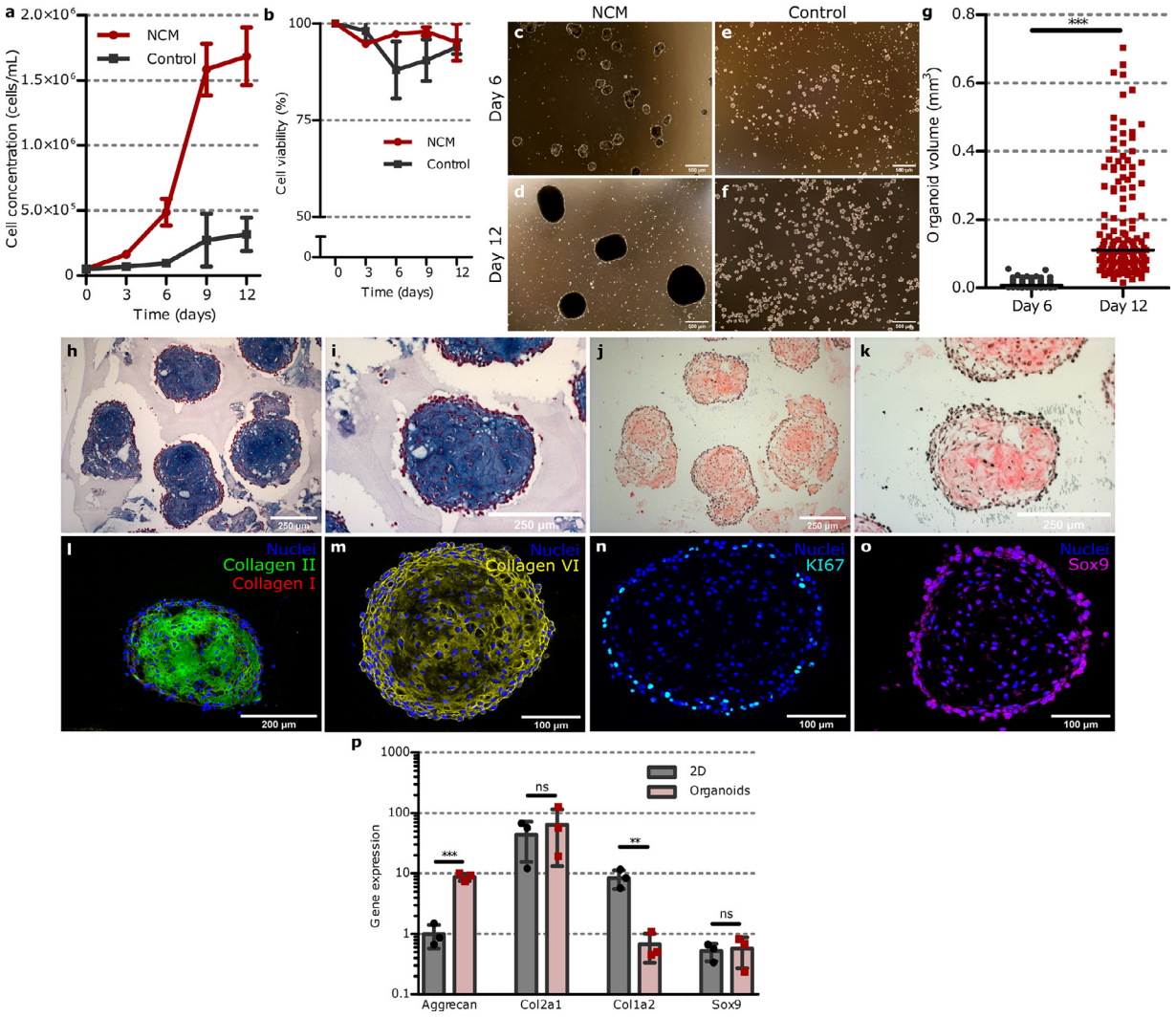

Fig. 1. Characterization of the organoids produced in the spinner flask. a, Cell proliferation in the spinner flasks with and without NCM over the period of 12 days (mean ± standard deviation) ($n = 3$ donors). **b**, Cell viability inside the spinner flasks with and without NCM over the period of 12 days (mean ± standard deviation) ($n = 3$ donors). **c-f**, Light microscopy image of the organoids cultured with or without NCM after 6 and 12 days (scale bar is 500 µm). **g**, Organoid volume distribution at day 6 and 12 inside the spinner flaks with NCM (median) ($n > 100$). **h-i**, Alcian blue staining of the organoids after 12 days of culture inside the spinner flaks with NCM (scale bar is 250 µm). **j-k**, Pricosirius Red staining of the organoids after 12 days of culture inside the spinner flaks with NCM (scale bar is 250 µm). **l**, Collagen type I (red) and type II (green) immunostaining on the organoids after 12 days of culture inside the spinner flask with NCM (scale bar is 200 µm). **m**, Collagen type VI (yellow) immunostaining on the organoids after 12 days of culture inside the spinner flask with NCM (scale bar is 100 µm). **n**, KI67 (cyan) immunostaining on the organoids after 12 days of culture inside the spinner flask with NCM (scale bar is 100 µm). **o**, Sox9 (magenta) immunostaining on the organoids after 12 days of culture inside the spinner flask with NCM (scale bar is 100 µm). **p**, Gene expression of chondrocytes expanded in 2D and of chondrocytes in the organoids after 12 days culture (mean ± standard deviation) ($n = 3$). All immunofluorescence pictures **l-o**, were counterstained with DAPI (blue). *, **, *** and ns indicate p ⟨ 0.05, $p < 0.01$, $p < 0.001$ and p ⟩ 0.05 respectively.

After 12 days, there was a 34 ± 4 fold increase in cell number in the group with NCM, while in the group without NCM there was only a 6 ± 2 fold increase. The cell growth curve was composed of three phases: a lag phase during the first 3 days, exponential phase between day 3 and 9, and stationary phase which took place after day 9 probably due to insufficient medium refreshment. Cell viability remained always above 88% for both conditions throughout the culture period (Fig. 1b). The organoid concentration after 12 days was 56.2 ± 21.6 organoids/mL ($n = 3$ donors). After 6 days of culture, cells cultured with NCM had already self-assembled into small organoids (cells and ECM constituents from the NCM) with a diameter of approx. 260 µm (Fig. 1c). These organoids kept growing reaching 600 µm in diameter at day 12. (Fig. 1d). In contrast, in the group without NCM, cells aggregated to each other forming small aggregates (only cells), that stayed relatively the same in size over time (Fig. 1e-f). The growth of the organoids from day 6 to day 12 corresponded to an increase in the organoid's volume of 15.4 times. (Fig. 1g). We observed that the organoids were composed of charged glycosaminoglycans (Fig. 1h-i) and collagen (Fig. 1j-k) (Fig. A.2). And that the collagen network within the organoids was mainly composed of collagen type II, with little content of collagen type I (Fig. 1l) (Fig. A.3), similarly to the composition of NCM (Fig. A.4). We confirmed that there was no presence of collagen type X within the organoid's matrix (Fig. A.5). Hypertrophic chondrocytes were used as control (Fig. A.6). Within the ECM of cartilage, the chondrocytes are surrounded by a specialized matrix called pericellular matrix (PCM), primarily composed of collagen type VI [21]. The PCM plays a pivotal role in biomechanical signal transduction to the chondrocytes and therefore, in cartilage homeostasis [22,23]. Staining against collagen type VI, confirmed its presence and localization around the cells in the organoids confirming the presence of a structural PCM within the organoids ECM (Fig. 1m) (Fig. A.7). Furthermore, the collagen type II was more concentrated in the interterritorial matrix between the

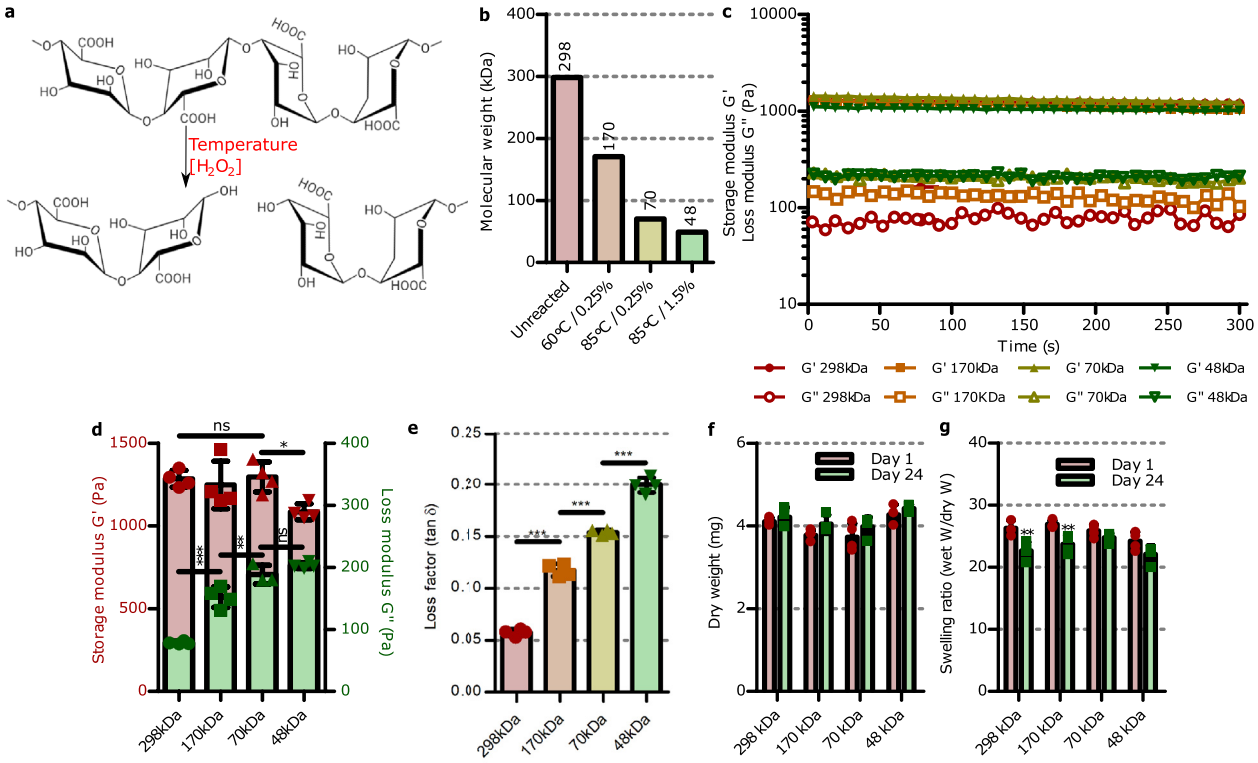

Fig. 2. Mechanical characterization of the alginate hydrogels. a, Illustration of the approach to fabricate alginate with different molecular weights by controlling the temperature of the reaction and the concentration of H_2O_2. **b**, Molecular weight measurements with GPC of the alginates obtained from the reaction with H_2O_2. **c**, Dynamic time sweep of the different alginate hydrogel formulations. **d**, Storage modulus (G', red) and loss modulus (G", green) of the different alginate hydrogel formulations ($n = 4$). **e**, Loss factor of the different alginate hydrogel formulations ($n = 4$). **f**, Dry weight of the alginate hydrogels at day 1 and day 24 of culture ($n = 4$). **g**, Swelling ratio of the alginate hydrogels at day 1 and day 24 of culture ($n = 4$). All data is plotted as mean ± standard deviations. *, **, *** and ns indicate $p\langle 0.05$, $p < 0.01$, $p < 0.001$ and $p\rangle 0.05$ respectively.

PCMs (Fig. 1l). After observing that the cell distribution was different within a organoid, as there was more cells in the outer region than in the core of the organoids, we hypothesized that cell proliferation was different as well. We stained for KI67, a protein present in proliferating but absent in resting cells, in order to detect dividing cells [24]. We observed that only the cells in the outside of the organoids were KI67 positive and that the cells in the core did not express this proliferation marker (Fig. 1n) (Fig. A.8). We stained against Sox9 to confirm the chondrogenic phenotype of the cells in the organoids and observed that all cells in the organoids were Sox9 positive (Fig. 1o) (Fig. A.9). Lastly, we compared the gene expression of the organoids after 12 days of culture inside the spinner flask with chondrocytes expanded in 2D for 12 days (Fig. 1p). We observed that the expression of aggrecan was 8.7 ± 1 times higher in the organoids when compared with the chondrocytes in 2D. The expression of collagen type II was slightly higher in the organoids than in 2D but this difference was not statistical significant. In contrast, the expression of collagen type I was 12.6 ± 4.2 times higher in the chondrocytes expanded in 2D when compared with the organoids. There was no difference in the expression of Sox9 between the 2D chondrocytes and organoids, and the expression of matrix metalloprotease 13 (MMP-13), aggrecanase 5 (ADAMTS5) and interleukin 1β (IL-1β) genes were not detected for both groups. Altogether, this data shows that NCM leads to massive proliferation of chondrocytes in the spinner flask while maintaining a viability above 95%. During the 12 days of culture, the chondrocytes and the ECM matrix from the NCM self-assembled into organoids that increase in number and size throughout the culture period. These organoids were composed of GAGs and collagen type II similar to native cartilage. Additionally, these organoids were organized into an interterritorial matrix rich in collagen type II and a PCM rich in collagen type VI with the cells located inside structures resembling lacunae. When compared with the standard 2D expansion system, organoids had higher expression of aggrecan and significantly lower expression of collagen type I.

3.2. Fabrication of hydrogels with different viscoelasticity

After establishing a system to produce cartilage organoids, we aimed at developing large scale tissues by encapsulating these organoids into hydrogels that would allow the growth and fusion of the organoids and lead to the generation of a homogenous tissue identical to native cartilage. We chose alginate as a mode hydrogel because its viscoelastic properties can be modulated independently of its elastic, swelling and degradation properties [25,26]. Hydrogels were fabricated with alginate of different molecular weights to modulate the viscous properties of the hydrogel, while the concentration of the crosslinker ($CaSO_4$) was adjusted so that the elastic properties did not significantly change. In order to fabricate alginate with different molecular weight, we reacted the alginate with hydrogen peroxide (H_2O_2) for 2 h which leads (Fig. 2a) to oxidation of the alginate chains resulting in an alginate with lower molecular weight without compromising its ability to gel (Fig. 2a) [27,28]. Increasing the reaction temperature and the volumetric concentration of H_2O_2 led to the fabrication of alginates with lower molecular weight (Fig. 2b). Hydrogels were fabricated by mixing a 2.5% (w/v) of 298, 170, 70 and 48 kDa alginate solution with 125.0, 166.5, 212.5 and 275.0 mM of $CaSO_4$ (Fig. A.10) and dynamic time sweep test was performed to characterize their viscoelastic behavior (Fig. 2c). We observed that the elastic component (G') of the different alginate hydrogel formulations was identical between groups (Fig. 2d, red bars), whereas the

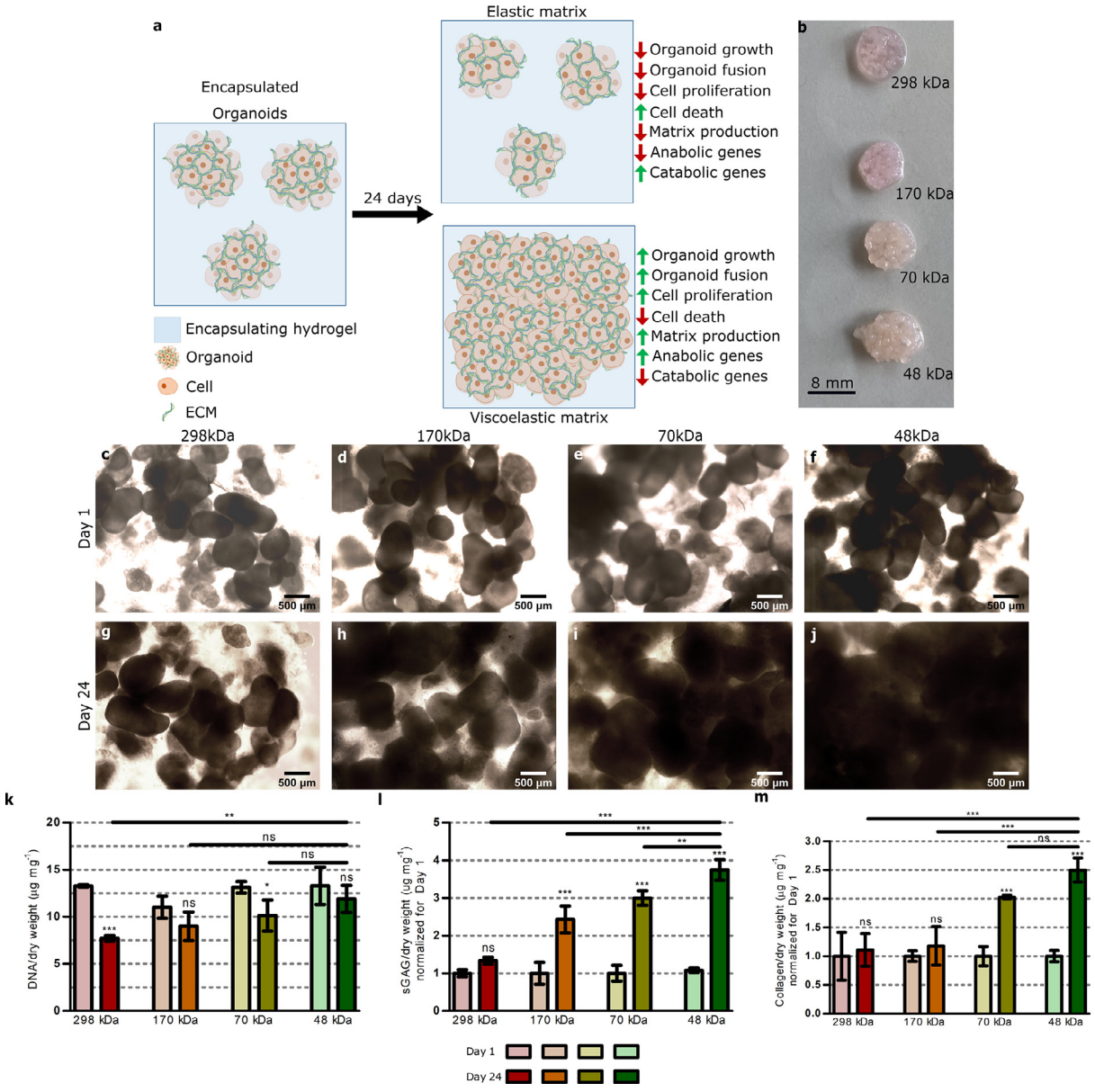

Fig. 3. Characterization of the morphology and biochemical content of the different alginate hydrogel formulations with organoids. a, Illustration of the effect viscoelasticity has on the growth and fusion of the organoids. b, Gross morphology of the different alginate hydrogel formulations with organoids after 24 days of culture (top to bottom: 298, 170, 70 and 48 kDa hydrogel formulations) (Scale bar is 8 mm). c-f, Light microscopy pictures of the different alginate hydrogel formulations with organoids after 1 and 24 day of culture (scale bar is 500 µm). k, DNA quantification in the different alginate hydrogel formulations with organoids after 1 and 24 days of culture ($n = 4$). l, GAG quantification in the different alginate hydrogel formulations with organoids after 1 and 24 days of culture ($n = 4$). m, Collagen quantification in the different alginate hydrogel formulations with organoids after 1 and 24 days of culture ($n = 4$). Data in k-m is represented as mean ± standard deviations and normalized for the dry weight of the hydrogel. *, **, *** and ns indicate p ⟨ 0.05, $p < 0.01$, $p < 0.001$ and p ⟩ 0.05 respectively.

viscous component (G'') increased as the molecular weight of the alginate decreased (Fig. 2d, green bars). The G'' was 78.3 ± 2.4 for the 298 kDa hydrogel formulation and 202.9 ± 4.6 for the 48 kDa hydrogel formulation. The loss factor, that describes the ratio between the viscous and the elastic component of the hydrogel, increased as the molecular weight decreased (Fig. 2e). The loss factor was 0.057 ± 0.003 for the 298 kDa formulation and 0.200 ± 0.008 for the 48 kDa formulation. Next, we characterized the degradation rate and swelling properties of the different hydrogel formulations after 1 and 24 days of culture. We observed that the dry weight for all formulations was identical between groups and there was no significant degradation of the hydrogels during the 24 days of culture (Fig. 2f). In terms of swelling properties, there was no significant difference between the hydrogel formulations at day 1 and 24. In sum, we fabricated four different alginate formulations with similar elastic properties (G'), but different viscous properties (G'') and therefore different viscoelastic behavior (tan δ). These formulations were mechanically stable, with negligible loss of dry weight and minor changes in the swelling properties (Table A.1). This development allowed us to investigate how viscoelasticity of the matrix affected neocartilage formation by the organoids produced in the spinner flask with NCM.

3.3. Matrix viscoelasticity affects cartilage formation by the organoids

We then investigated the impact that matrix viscoelasticity has on cartilage formation by the organoids (Fig. 3a). After 24 days of culture, the gross morphology of the hydrogels was drastically dif-

ferent among groups (Fig. 3b). In the 298 and 170 kDa hydrogel formulations, the volume of the hydrogel did not change during the culture period while in the 70 and 48 kDa formulations the volume of the hydrogel increased, as the constructs grew in width and height. We observed that the organoid concentration inside the hydrogels was identical among the groups at day 1 (Fig. 3c-f). After 24 days of culture, nothing changed for the most elastic hydrogel formulation (298 kDa), as it was still possible to identify the individual organoids and there was no filling of the initial empty space inside the hydrogel with new cells and matrix (Fig. 3e). For the 170 kDa formulation hydrogel, the initial empty space inside the hydrogel started to be filled with cells and matrix. However, it was still possible to identify single organoids, meaning that they were not actually fusing together. On the other hand, for the 70 and 48 kDa hydrogel formulations, most of the empty space inside the hydrogel was filled with cells and matrix and the organoids fused together creating a more homogenous tissue (Fig. 3i-j). From the DNA analysis, we observed that there was a reduction in DNA content for all hydrogel formulations from day 1 to day 24 (Fig. 3k). In the more elastic formulation (298 kDa), there was a reduction of 42 ± 2.0% in DNA content per dry weight from day 1 to day 24. For the other formulations, the reduction in DNA content was less pronounced with a reduction of 18.5 ± 11.3%, 22.8 ± 10.9%, and 10.5 ± 9.4% for the 170, 70 and 48 kDa hydrogel formulations respectively (Fig. A.11a). In terms of charged GAG content, we observed an increase in the amount of charged GAGs from day 1 to day 24 for all conditions, with an increase in production as the viscosity of the hydrogel increased (Fig. 3l). There were fold increases of 1.3 ± 0.1, 2.4 ± 0.4, 3.0 ± 0.2 and 3.8 ± 0.3 for the 298, 170, 70 and 48 kDa hydrogel formulations (Fig. A.11b). The production of collagen was also affected by the viscoelasticity of the matrix (Fig. 3m). In the more elastic hydrogel formulations, there was no significant production of collagen. On the other hand, in the more viscous hydrogels, there were fold increases of 2.0 ± 0.0 and 2.5 ± 0.2 for the 70 and 48 kDa hydrogel formulations (Fig. A.11c).

We analyzed the composition of the four hydrogel formulations by histology and immunostaining. At day 1 the composition of the different alginate hydrogels was identical as expected, with single isolated organoids made of cells, collagen type II and VI and GAGs. Immunostaining confirmed that after 24 days there was no filling of the initial empty space with new cells and matrix in the 298 and 170 kDa alginate hydrogels (Fig. 4e-f; m-n; u-v). After the culture period, the characteristic outer region of the organoids was less smooth and with less cells, suggesting degradation of the matrix during the culture period. In contrast, for the more viscous hydrogel formulations (70 and 48 kDa), after 24 days of culture, there was fusion of the organoids, due to filling of the initial empty space with cells and new matrix. The new matrix formed during the culture period was mainly composed of collagen type II, type VI and GAGs (Fig. 4g-h; o-p; w-x). From all the alginate hydrogel formulations tested, the formulation with higher viscosity (48 kDa) performed the best in terms of formation of new cartilage (Fig. A.12). Afterwards, we confirmed that the cells in all hydrogel alginate formulations were Sox9 positive after 24 days of culture (Fig. A.13) and that there was no production of collagen type X (Fig. A.14).

We also evaluated the gene expression in the different hydrogel alginates after 1 and 24 days of culture (Fig. 5). The gene expression in the organoids after 12 days of culture in the spinner flask and before encapsulation was used as baseline for aggrecan, collagen type II and I, and Sox9. We observed that one day after encapsulation, the expression of aggrecan decreased for all formulations (Fig. 5a). The expression continued to decrease during the culture period for all formulations except the 48 kDa hydrogel which was restored to high levels. The expression of collagen type II also decreased after encapsulation in all hydrogel formulations and remained low throughout the culture period for the 298 and 170 kDa hydrogels (Fig. 5b). In contrast, in the 70 and 48 kDa hydrogels, the expression increased between day 1 and 24, with the highest collagen type II gene expression being reported for the 48 kDa alginate hydrogel. The expression of collagen type I during the 24 days stayed negligible, identical to the levels pre-encapsulation (Fig. 5c). Sox9 expression also decreased after encapsulation, and significantly increased during the 24 days of culture only in the 48 kDa hydrogel (Fig. 6d). Encapsulation of the organoids led to the upregulation of catabolic genes that were not detected within the organoids before encapsulation. Expression of MMP-13 and ADAMTS5 were detected one day after encapsulation for all formulations (Fig. 6e-f). The expression was higher in the 298 kDa hydrogel and decreased as the viscosity of the hydrogels increased. After 24 days of culture, MMP-13 and ADAMTS5 expression were negligible in all formulations. IL-β1 expression was also upregulated after encapsulation, with higher expression in the more elastic formulations (Fig. 6g). In conclusion this data shows that the viscoelasticity of the matrix deeply affects the formation of cartilage by the organoids. We identified an alginate formulation with a loss of tangent of 0.2 that was optimal for cartilage formation, as it promoted the growth and fusion of the organoids by enhancing proliferation, migration and matrix synthesis of the cells while at the same time downregulated the expression of catabolic genes. These constructs had an interconnected matrix similar to native cartilage in composition and organization.

3.4. Organoid encapsulation leads to superior cartilage compared to single cells

After confirming that encapsulation of organoids in hydrogels with suitable viscoelastic properties led to the formation of cartilage like tissues, we also compared this new methodology with the standard approach. The standard approach to produce in vitro cartilage consists of expanding chondrocytes in 2D monolayer and then encapsulating them into a hydrogel. We expanded chondrocytes in 2D and then encapsulated them into the 48 kDa alginate hydrogel as single cells to compare with organoids encapsulation in terms of cartilage formation (data in Section 3.3; Fig. 3k-m). DNA analysis showed that there was similar content at day 1 and day 24 in the hydrogels with single cells and organoids (Fig. 6a). In terms of GAG content, there was an increase for both groups during the culture period, reaching similar levels at day 24 (Fig. 6b). The collagen content also increased in both groups during the culture period (Fig. 6c). In the hydrogels with single cells there was an increase from 2.3 ± 0.9 (day 1) to 51.1 ± 7.4 (day 24) µg/mg, which corresponds to a 6.4 ± 0.8 fold increase in collagen content. In the hydrogels with organoids, the collagen content increased from 37.8 ± 3.7 (day 1) to 94.5 ± 7.9 (day 24), corresponding to a fold increase of 2.5 ± 0.2. During the 24 days of culture the increase in collagen was higher for the hydrogels with single cells, however at the end of the 24 of days of culture, the hydrogels with organoids had 1.8 ± 0.1 times more collagen than the hydrogels with single cells. Next, we assessed the type of collagen present within the tissue construct. We observed that in the hydrogels with single cells, there was presence of both collagen type I and type II (Fig. 6d), in contrast to the hydrogel with organoids which had undetectable levels of collagen type I (Fig. 6e). This different behavior is likely a consequence of the 2D expansion step before encapsulation, as we showed that cells expanded in 2D have higher gene expression of collagen type I and lower expression of collagen type II than cells in the organoids inside the spinner flask. Hydrogels with single cells and organoids had similar amounts of collagen type VI (Fig. 6f-g) and GAGs (Fig. 6h-i). Afterwards we evaluated if the matrix formed during the culture period was sufficient and

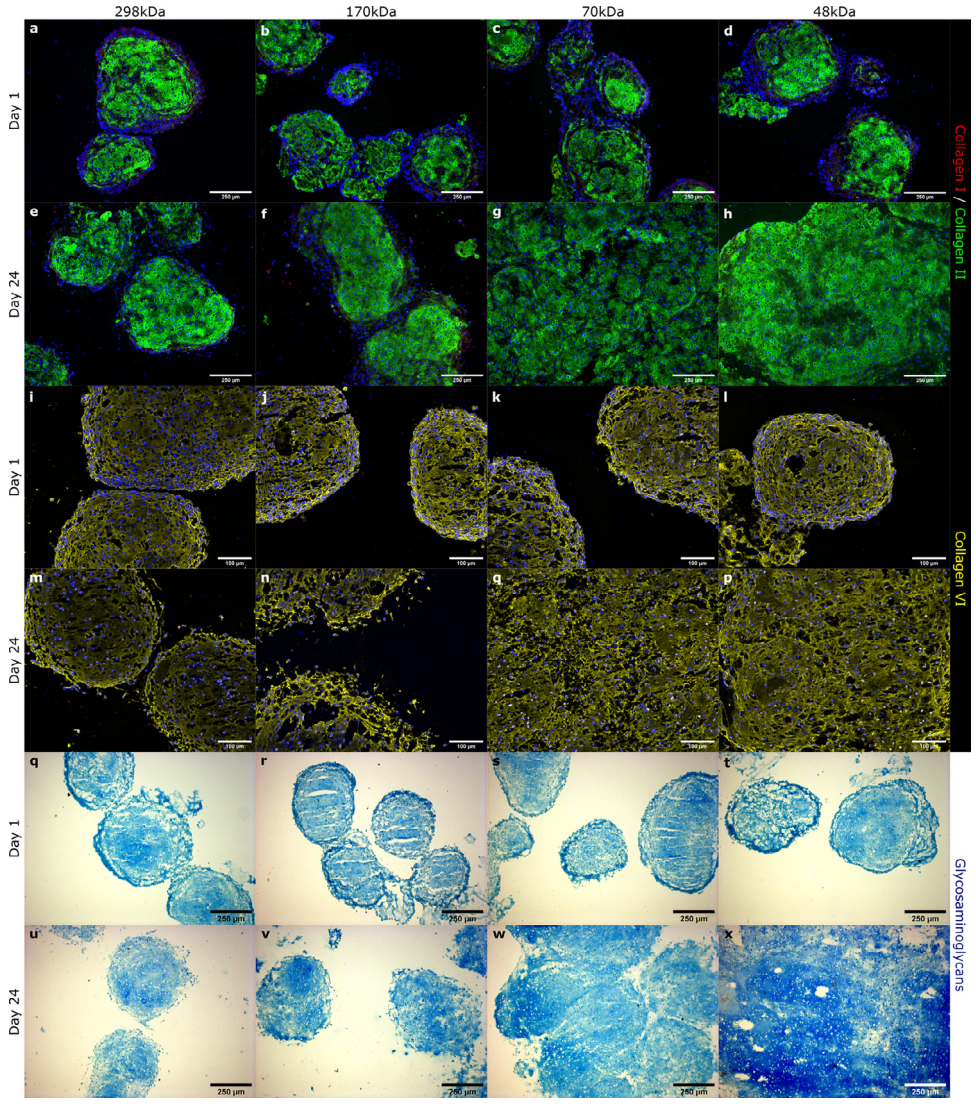

Fig. 4. Matrix composition in the different hydrogel formulations after 1 and 24 days of culture. a-h, Antibody staining against collagen type I (red) and type II (green) in the different alginate hydrogel formulations after 1 and 24 days of culture (scale bar is 250 μm). **i-p**, Antibody staining against collagen type VI (yellow) in the different alginate hydrogel formulations after 1 and 24 days of culture (scale bar is 100 μm). **q-x**, Alcian blue staining against glycosaminoglycans in the different alginate hydrogel formulations after 1 and 24 days of culture (scale bar is 250 μm). Cell nuclei was stained with DAPI in the pictures **a-p**.

mechanically stable to keep the integrity of the tissue construct after removal of the alginate network. The tissue constructs were placed in a buffer that dissolves the alginate hydrogel matrix by competing for the ions that hold the alginate chains together. We used the most elastic alginate hydrogel (298 kDa) with organoids as negative control because no interconnected matrix is formed in this group during the culture period. In the 298 kDa hydrogel, dissolution of the alginate network compromised the integrity of the tissue construct as it started falling apart leading eventually to the release of organoids into the buffer (Fig. 6j, first row). In contrast, in the more viscoelastic hydrogel (48 kDa), removal of the alginate network did not affect the integrity of the tissue construct for both organoids (Fig. 6j, second row) and single cells (Fig. 6j, third row) groups. This demonstrates that the interconnected matrix formed during 24 days in the 48 kDa hydrogel was sufficient to hold the tissue construct together. In the conclusion, this data shows that cartilage formation is enhanced by encapsulating organoids rather than single cells, as it leads to the formation of more matrix with higher quality (only collagen type II). This matrix was mechanically stable and capable of alone holding the tissue construct together after removal of the alginate network.

4. Discussion

To our knowledge, we describe here for the first time a methodology to generate bovine cartilage organoids in large scale (thousands of organoids per 125 mL in one spinner flask) and within two weeks, through a self-assembly process between cells and ECM constituents. To avoid the downsides associated with the 2D expansion of chondrocytes, researchers have employed a variety of 3D culture systems (e.g. pellets, spheroids, microtissues) that enhance the viability and the chondrogenic potential of chondrocytes. The constructs obtained using the 3D approaches can then be encapsulated into hydrogels to achieve the formation of cartilage that is superior in quantity and quality when compared with the use of single cells expanded with the conventional 2D systems [29–33]. However, these approaches also have some disadvantages: they do not necessarily yield a higher cell number than 2D systems [34]; they can be technically challenging and laborious with the need for microfabrication equipment/steps to generate 3D culture of chondrocytes and challenges with purification. Finally, they cannot be efficiently scaled up and therefore have very limited applicability to joint-sized cartilage-tissue engineering therapies. Spinner flasks

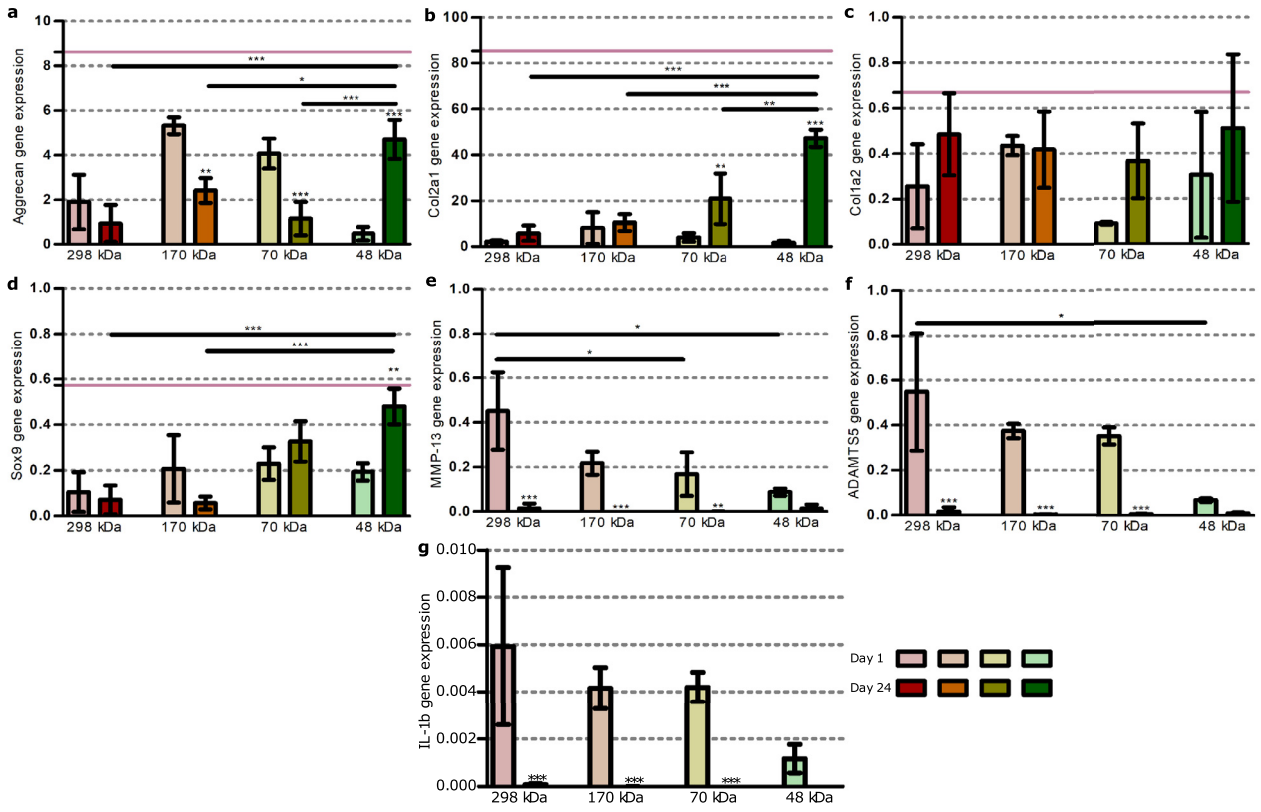

Fig. 5. Genetic profile of the organoids in the different alginate hydrogels formulations. a-g, Gene expression of aggrecan, collagen type II, collagen type I, Sox9, MMP-13, ADAMTS5 and IL-1β inside the alginate hydrogels after 1 and 24 days of culture. The pink line in the graphs **a-d** represent the mean expression of the gene in the organoids after 12 days of culture in the spinner flask just before encapsulation. All data is plotted as mean ± standard deviations ($n = 4$). *, **, *** indicate $p < 0.05$, $p < 0.01$ and $p < 0.001$ respectively.

have been widely used to form and culture organoids and have unique features such as easy handling, high throughout and are easy to scale up [35–37]. Our methodology of culturing chondrocytes in a spinner flask with NCM led to the production of self-assembling organoids similar in organization and composition to native cartilage. These organoids consisted of a core with spaced cells residing in lacunae like structures and surrounded by a collagen type VI rich PCM within a collagen type II and GAG rich interterritorial ECM. The organoid's core was surrounded by a border with higher cell density due to active proliferation of the cells, and where the cells had cell to cell contact with their neighboring cells. Within 12 days of culture, we were able to achieve a 34 ± 4 fold increase in cell number and the production of thousands of organoids without the addition of any growth factor to the culture medium. Since organoid formation occurred within 6 days only in the group with solubilized NCM, their volume increased by 15 times between day 6 and day 12, and they were composed of GAGs and collagen type II similarly to NCM, we can conclude that the ECM constitutions from NCM are crucial for the formation and growth of the organoids [38–40]. Recently, a similar approach has been used to generate liver inside spinner flaks through a self-assembly process between cells and ECM proteins [41]. In that study, Matrigel was added to the culture medium and used as source of ECM for the generation of the organoids. Throughout the culture period cell viability was higher than 88%, however the protocol used might per se have an impact on the measured viability. Prior to measuring cell viability, the samples were enzymatically digested with hyaluronidase and collagenase to release the cells for counting. Enzymatic digestion with these two enzymes is known to affect the viability of chondrocytes, and therefore the actual viability of the cells inside the spinner flask is likely to be higher than the one actually measured, for both cultures, i.e. with and without NCM [42,43]. In terms of gene expression, the cells in the organoids had higher expression of aggrecan and lower expression of collagen type I than the cells in 2D monolayer culture. There was no statistical difference for Sox9 and collagen type II gene expression between the two groups. It is known that culture of chondrocytes in 2D monolayers reduces the expression of relevant chondrogenic genes, and that this effect is more pronounced at higher cell passages [44,45]. For bovine chondrocytes it has been shown, that after one passage there is a significant reduction in aggrecan and Sox9 and a significant increase in collagen type I gene expression when compared with cells not passaged. While collagen type II gene expression is significantly reduced only after two passages [45]. These effects became more pronounced as the cells are subjected to more passages. In our study we cultured low passage cells (P1) in monolayer for the 2D control group in order to minimize their de-differentiation. This might explain why cells in the organoids and cells in 2D have similar expression of collagen type II and Sox9, as the cells in monolayer might still conserve their normal expression for these two genes. In addition to that, a previous study from our group showed that NCM per se does not induce collagen type II gene expression in chondrocytes [15]. Other study also reported no difference in collagen type II gene expression between low passage (P2) bovine chondrocytes cultured as aggregates or monolayer in chondrogenic expansion medium [32]. Our methodology is a technically simple strategy to produce organoids that can be easily scaled up, by increasing the working volume of the flask or the number of flasks, as it only requires the addition of NCM, and therefore high yields of cell numbers can

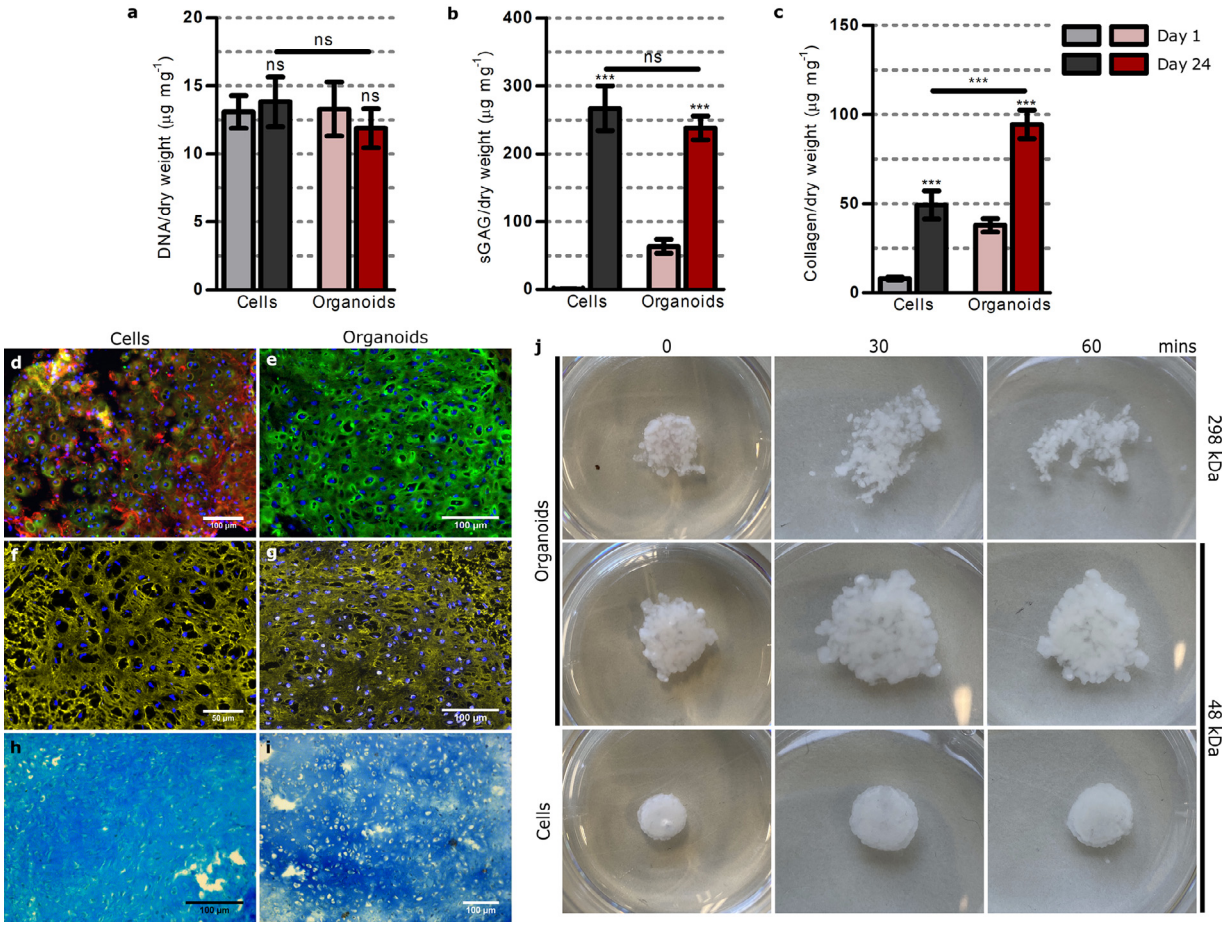

Fig. 6. Cartilage formation by single cells and organoids in the more viscoelastic alginate hydrogel. a-c, Biochemical analysis of DNA, GAG and collagen in the 48 kDa alginate hydrogel with single cells and with organoids after 1 and 24 days of culture ($n = 4$). Data is represented as mean ± standard deviations and normalized for the dry weight of the hydrogel. *** and ns indicate $p < 0.001$ and $p > 0.05$ respectively. **d-e**, Antibody staining against collagen type I (red) and type II (green) after 24 days of culture. **f-g**, Antibody staining against collagen type VI (yellow) after 24 days of culture. **h-i**, Alcian blue staining against glycosaminoglycans after 24 days of culture. Cell nuclei was stained with DAPI in the pictures **d-g. j**, Pictures of the 298 kDa alginate hydrogel with organoids (first row), 48 kDa alginate hydrogel with organoids (second row) or single cells (third row) in the alginate disassociation buffer after 0 (first column), 30 (second column) and 60 (third column) minutes of incubation. .

be obtained which are necessary for joint-sized tissue engineering therapies [46]. Other groups have employed dynamic suspension cultures to expand chondrocytes and other cell types with the use of microcarriers, such as mesenchymal (MSCs) or adipose derived stromal cells (ADSCs) for cartilage tissue engineering [47–51]. Culture of cells with microcarriers inside spinner flasks is an attractive approach because of its higher surface area per unit volume of media when compared with T-flask culture [52]. However, it still relies in the attachment of the cells to the surface of the microcarriers where they can grow as monolayers. Consequently, chondrocytes expanded with microcarriers in spinner flasks still produce much collagen type I once they are cultured as a pellet or encapsulated into hydrogels [47,51,53]. In our study, we explored a new strategy based on the self-assembly between cells and ECM constituents to expand chondrocytes and form organoids inside spinner flasks. The organoids produced in this study had very little expression of collagen type I when compared with chondrocytes expanded in 2D, and this translated into the formation of a tissue with no detectable levels of collagen type I once the organoids were encapsulated into a hydrogel. This demonstrates the advantage of our new approach over the expansion of chondrocytes in monolayers, whether it is on the surface of microcarriers or tissue culture plastic. In this study we used juvenile bovine chondrocytes which are known for their high proliferative capacity. It is expected that the use of human chondrocytes will lead to lower cell yields, as these cells are known be less proliferative [54]. Future work will focus on using the methodology described here to expand human chondrocytes and compare it with other approaches described in literature. The influence that culture parameters (e.g. agitation speed, initial cell density or dosage regime) have on organoid formation and their size should also be investigated in order to maximize the yield, efficiency and determine the versatility of this methodology [55]. NCM might present several theoretical drawbacks due to its animal origin, such as poor characterization, possible batch-to-batch variability and the risk of disease transmission. It is of importance to identify which and at what concentrations, ECM molecules and bioactive factors (e.g. growth factors) in the NCM play a role in the process of organoid formation and developed a defined synthetic medium that can replace the NCM. Proteomic, inhibition and depletion studies can help to elucidate the key components of NCM's bioactivity. In our study, during the production of NCM, we did not remove residual DNA which is known to act in vivo as a damage-associated molecular pattern (DAMP) [56]. However, previous work using this NCM processing method showed no upregulation of inflammatory and catabolic genes on the treated cells [15]. Nevertheless, for clinical purposes, removal of residual DNA from NCM should be explored and its impact on NCM's bioactivity investigated.

The second objective of this study was to use these organoids and assemble them inside a hydrogel to produce large scale tissues

resembling neocartilage. Hydrogels have been widely used for cartilage tissue engineering and a detailed review can be found elsewhere [57]. The influence of hydrogel properties such as elasticity, swelling and fixed charge on chondrocyte behavior has also been reported [58–61]. However, one mechanical property often neglected is viscoelasticity of the matrix. The living tissues in our body are viscoelastic materials, and viscoelasticity is a critical parameter capable of affecting cell behavior and tissue/organ homeostasis, regeneration and disease progression [25,26,62–67]. It was recently shown that viscoelasticity of the matrix plays a pivotal role at the cellular level in chondrocyte behavior and cartilage formation [25,68]. We hypothesized that viscoelasticity of the hydrogel would also have a critical effect on the growth and fusion of the organoids. Although an elastic matrix would constrain the organoids' growth and fusion, a hydrogel with suitable relaxing properties would offer minimal resistance to the growth of the organoids, cell proliferation, migration, matrix production and ultimately to the generation of a homogenous cartilage like tissue. We chose alginate as a model hydrogel to study how viscoelasticity of the matrix affects cell and organoid behavior, because the relaxation of alginate hydrogels can be controlled independently of the elasticity without affecting other properties of the hydrogel. When combined with divalent ions (e.g. Ca^{2+}), the alginate will gel due to the formation of weak ionic crosslinks, which under stress or strain can dissociate and reform again elsewhere, leading to the plastic deformation of the hydrogel [69]. The viscoelastic properties of the resulting hydrogel can be modulated by using different molecular weight alginates in combination with different concentrations of crosslinker which will result in altered connectivity and polymer chain mobility. Lowering the molecular weight leads to an increase in the viscosity and decrease in the elasticity of the resulting hydrogel. The reduction in elasticity can be compensated by adjusting the concentration of the crosslinker without interfering in the viscosity. This allows the fabrication of hydrogels with different viscosity but with similar elasticity and therefore different viscoelastic behavior [26]. Cartilage matrix deposition is not correlated with the concentration of calcium crosslinker [25]. By tuning the molecular weight of alginate and the crosslinker concentration, we fabricated four different formulations that had similar elasticity, but different viscosity and therefore different viscoelastic behavior without altering their swelling and degradation properties. Once the organoids were encapsulated into these alginate hydrogels, we observed a drastically different behavior among the tested groups, with a positive correlation between viscoelasticity and cartilage formation. Elastic hydrogels (298 and 170 kDa) constrained the growth and fusion of the organoids, inhibiting the development of neocartilage tissue. In contrast, viscous hydrogels (70 and 48 kDa) allowed the growth of the organoids by enhancing cell proliferation, migration and matrix deposition This ultimately led to the fusion of the encapsulated organoids and the development of a stable and homogenous tissue similar to native cartilage in composition and organization that was composed of GAGs and collagen type II and type VI. We did not detect any collagen type I or type X in any formulation tested. Gene expression analysis showed that encapsulation in the alginate lead to a reduction in the expression of aggrecan, collagen type II and Sox9 by the organoids. This might be a consequence of the encapsulation procedure and/or a change in the microenvironment sensed by the organoids such as the new mechanical properties imposed by the alginate network, the absence of shear forces caused by the agitation in the spinner flask or absence of NCM in the medium. Lee *at al.* (2017) observed that encapsulation of bovine chondrocytes in alginate hydrogels decreased the expression of certain genes when compared with chondrocytes in native cartilage [25]. Gene expression analysis also showed that elastic hydrogels upregulated catabolic enzymes, such as MMP-13 and ADAMTS5 as early as day 1. Additionally, we observed an higher expression of the IL-1β gene for the more elastic hydrogel formulations. This suggests that the expression of MMP-13 and ADAMTS5 might be activated through the IL-1β pathway, as it is known that this pathway controls the expression of catabolic genes in OA [70,71]. This data is in agreement with the findings that purely elastic hydrogels upregulate the expression of catabolic genes in encapsulated chondrocytes, while viscous formulations downregulate it [25]. A consequence of the expression of these catabolic enzymes was the degradation of outer border of each organoid. After 24 days of culture, the outer border of each organoid was less smooth, presented signals of destruction and had far less cells than at day 1 for the 298 and 170 kDa hydrogel formulation. The expression of these genes was lowest for the more viscoelastic hydrogel (48 kDa). There was a decrease during the culture period in the expression of the catabolic enzymes for all the hydrogel formulations tested. It is very likely that the expression of these catabolic enzymes is solely coming from the cells in the outer border of the organoid, that are in direct contact with the alginate network. And that the cells in the core of the organoid do not express these catabolic enzymes, as we did not observe any degradation of the ECM or cell death in the core of the organoid. The mechanisms that cells use to create a suitable microenvironment is highly depended on the mechanical properties of the surrounding matrix. Raeber et al. (2005) showed that cell migration within MMP-sensitive PEG matrices was greatly affected by MMP modulators [72]. The absence of MMP sensitive domains in those PEG matrices impaired cell migration. On the same study, the authors observed that cell migration in collagen and fibrin hydrogel was insensitive to MMP activity, because the cells could rearrange the surrounding hydrogel network, due to the viscoelastic behavior of collagen and fibrin. The cells in the organoids cannot degrade the alginate and therefore can only rearrange it if the alginate network behaves like a viscoelastic material. In the more elastic formulation (298 kDa), the cells cannot rearrange the surrounding alginate network and in response to that express high levels of catabolic enzymes. We also observe cell death in this formulation during the 24 days of culture, which occurs mainly in the outer area of the organoids. We hypothesized that in the more elastic hydrogel (298 kDa), the cells in the outer area of the organoids that produce catabolic enzymes at day 1, die during the culture period and this could explain the decrease in catabolic activity observed for this formulation. For the other alginate formulations, the cells can rearrange the surrounding hydrogel network, independently of MMP activity, creating a suitable space for their cellular processes, which might lead to a reduction in catabolic activity throughout the culture period. However, further studies are needed to elucidate the different behavior that the cells in the core and outer border of the organoids have in response to the physical properties of the encapsulating hydrogel. We also reported that the expression of anabolic genes such as aggrecan and collagen type II, and Sox9 reached a maximum in the most viscoelastic hydrogel formulation (48 kDa). The 48 kDa alginate hydrogel was the formulation that perform the best in terms of cartilage deposition. The viscoelasticity of this formulation was characterized with a loss factor of 0.2, which interestingly matches the loss factor reported for bovine cartilage [73]. In sum, viscoelasticity of the encapsulating hydrogel is pivotal for cartilage production and it should always be considered when developing new hydrogels systems for cartilage tissue engineering. Additionally, we showed that large scale homogenous neocartilage tissues can be obtained by simply encapsulating organoids, derived from bovine chondrocytes, into a hydrogel with the right viscoelastic properties, without the need of adding to the culture medium exogenous growth factors (e.g. TGF-β1/3 or BMP-2) or steroids (e.g. dexamethasone). However it is known that bovine chondrocytes have an higher synthetic capacity than human chondrocytes [32,74]. Therefore, future work should investigate if

the same behavior is observed in organoids derived from human chondrocytes, and if similar results can be obtained by simply tuning the viscoelasticity of the encapsulating hydrogel or if stimulation with exogenous growth factors is also required. Encapsulation of organoids also proved to be a superior strategy when compared with the standard approach of single cell encapsulation that were previously expanded in 2D. Organoid encapsulation resulted in higher production of new matrix and of better quality, as it was composed of collagen type II with no detectable levels of collagen type I; in contrast to the matrix formed by the encapsulated single cells, which consisted of a mixture of collagen type I and II. The fact that the cells in the organoids are within a 3D cellular niche similar to their native microenvironment can explain why once encapsulated they retain their normal synthetic capacity. In contrast, when the cells are expanded in 2D, they experience phenotypic drifts which result in the aberrant production of matrix once encapsulated [75–78]. Collagen makes up to about 60% of the dry weight of cartilage and juvenile bovine cartilage has been reported to have a collagen/GAG mass ratio of 1.9 [79,80]. After 24 days, the dry weight of the 48 kDa alginate hydrogel with organoids consists of 9.45 $\pm$ 0.45% collagen while the collagen/GAG mass ratio is 0.46 $\pm$ 0.08. In comparison, the dry weight of the 48 kDa alginate hydrogel with single cells consists of 4.92 $\pm$ 0.64% collagen and the collagen/GAG mass ratio is 0.19 $\pm$ 0.03 after 24 days. This shows that encapsulation of organoids leads to the formation of a tissue with an higher collagen content and collagen/GAG ratio than hydrogels with single cells. Since collagen type II is still highly expressed in the 48 kDa alginate hydrogel with organoids at day 24, future work should therefore investigate if culturing the constructs for longer periods will lead to a more mature tissue with higher collagen content and a higher collagen/GAG ratio. Or if addition of an extra stimulus (e.g. growth factor or mechanical stimulation) is required to reach values similar to the ones found in native cartilage. Here we show that assembly of the organoids in the right viscoelastic hydrogels can improve and accelerate the in vitro fabrication of cartilage. In this study we used bovine chondrocytes and therefore it is important that further studies assess the feasibility of using this approach with human chondrocytes. Once cartilage organoids derived from human chondrocytes are successfully developed, their potential in the treatment of cartilage lesions should be investigated with in vivo studies.

Overall, this methodology describes the production of cartilage bovine organoids and that their assembly in hydrogels with suitable viscoelastic properties leads to the formation of a homogenous tissue resembling native cartilage.

5. Conclusions

In summary, we developed a new methodology to expand chondrocytes in dynamic culture systems. This new methodology used NCM as medium supplement and led to the massive proliferation of chondrocytes and their self-assembly with the ECM constituents into organoids. These organoids were similar in composition and organization to native cartilage, with chondrocytes sitting inside lacunae, surrounded by a PCM rich in collagen type VI within an interterritorial ECM composed of collagen type II and GAGs. Gene expression analysis showed that with this system, it was possible to overcome the problems associated with 2D expansion, such as aberrant expression of collagen type I. Once encapsulated into hydrogels with suitable viscoelastic properties, these organoids grew and fused together creating a neocartilage tissue. This tissue was composed of collagen type II, GAGs and collagen type VI, and was mechanically stable. Here we showed that the use of organoids for cartilage tissue engineering is superior to the conventional method of expanding chondrocytes in 2D and then encapsulating them as single cells. Due to the similarities with native cartilage, these organoids on their own have the potential to revolutionize how cartilage research is performed, because they can be used as superior and more complex in vitro models to study signaling pathways, disease progression, tissue engineering or drug development. Furthermore, these organoids and their fast mass production combined with a key hydrogel characteristic, which up to now has not received much attention, have the potential to open the door for large scale cartilage regeneration such as for entire joint surfaces. Future work will focus on generating cartilage organoids derived from human chondrocytes, optimization of the protocol for organoid formation, and investigating the potential of human derived cartilage organoids in the treatment of cartilage lesions.

Declaration of Competing Interest

The authors declare the following financial interests/personal relationships which may be considered as potential competing interests

Acknowledgments

This study is supported by the partners of Regenerative Medicine Crossing Borders (RegMed XB), a public-private partnership that uses regenerative medicine strategies to cure common chronic diseases. This collaboration project is financed by the Dutch Ministry of Economic Affairs by means of the PPP Allowance made available by the Top Sector Life Sciences & Health to stimulate public-private partnerships

Supplementary materials

Supplementary material associated with this article can be found, in the online version, at doi:10.1016/j.actbio.2021.04.008.

References

[1] D.J. Hunter, S. Bierma-Zeinstra, Osteoarthritis, Lancet 393 (2019) 1745–1759, doi:10.1016/S0140-6736(19)30417-9.
[2] L.S. Lohmander, M. Gerhardsson de Verdier, J. Rollof, P.M. Nilsson, G. Engström, Incidence of severe knee and hip osteoarthritis in relation to different measures of body mass: a population-based prospective cohort study, Ann. Rheum. Dis. 68 (2009) 490–496, doi:10.1136/ard.2008.089748.
[3] World Health Organization, Priority Medicines For Europe and the World Update Report, 2013 (n.d.) https://www.who.int/medicines/areas/priority_medicines/Ch6_12Osteo.pdf?ua=1 (accessed July 21, 2020).
[4] J.R. Steadman, W.G. Rodkey, J.J. Rodrigo, Microfracture: surgical technique and rehabilitation to treat chondral defects, Clin. Orthop. Relat. Res. (2001) S362–S369, doi:10.1097/00003086-200110001-00033.
[5] B.M. Devitt, S.W. Bell, K.E. Webster, J.A. Feller, T.S. Whitehead, Surgical treatments of cartilage defects of the knee: systematic review of randomised controlled trials, Knee 24 (2017) 508–517, doi:10.1016/j.knee.2016.12.002.
[6] D. Saris, A. Price, W. Widuchowski, M. Bertrand-Marchand, J. Caron, J.O. Drogset, P. Emans, A. Podskubka, A. Tsuchida, S. Kili, D. Levine, M. Brittberg, Matrix-Applied Characterized Autologous Cultured Chondrocytes Versus Microfracture: two-Year Follow-up of a Prospective Randomized Trial, Am. J. Sports Med. 42 (2014) 1384–1394, doi:10.1177/0363546514528093.
[7] P. Niemeyer, D. Albrecht, S. Andereya, P. Angele, A. Ateschrang, M. Aurich, M. Baumann, U. Bosch, C. Erggelet, S. Fickert, H. Gebhard, K. Gelse, D. Günther, A. Hoburg, P. Kasten, T. Kolombe, H. Madry, S. Marlovits, N.M. Meenen, P.E. Müller, U. Nöth, J.P. Petersen, M. Pietschmann, W. Richter, B. Rolauffs, K. Rhunau, B. Schewe, A. Steinert, M.R. Steinwachs, G.H. Welsch, W. Zinser, J. Fritz, Autologous chondrocyte implantation (ACI) for cartilage defects of the knee: a guideline by the working group "Clinical Tissue Regeneration" of the German Society of Orthopaedics and Trauma (DGOU), Knee 23 (2016) 426–435, doi:10.1016/j.knee.2016.02.001.
[8] T. Minas, T. Bryant, The Role of Autologous Chondrocyte Implantation in the Patellofemoral Joint, Clin. Orthop. Relat. Res. (2005) 436 https://journals.lww.com/clinorthop/Fulltext/2005/07000/The_Role_of_Autologous_Chondrocyte_Implantation_in.6.aspx.
[9] W. Bartlett, J.A. Skinner, C.R. Gooding, R.W.J. Carrington, A.M. Flanagan, T.W.R. Briggs, G. Bentley, Autologous chondrocyte implantation versus matrix-induced autologous chondrocyte implantation for osteochondral defects of the knee: a prospective, randomised study, J. Bone Joint Surg. Br. 87 (2005) 640–645, doi:10.1302/0301-620X.87B5.15905.

[10] Y. Xiang, V. Bunpetch, W. Zhou, H. Ouyang, Optimization strategies for ACI: a step-chronicle review, J. Orthop. Transl. 17 (2019) 3–14, doi:10.1016/j.jot.2018.12.005.
[11] J. Diaz-Romero, J.P. Gaillard, S.P. Grogan, D. Nesic, T. Trub, P. Mainil-Varlet, Immunophenotypic analysis of human articular chondrocytes: changes in surface markers associated with cell expansion in monolayer culture, J. Cell. Physiol. 202 (2005) 731–742, doi:10.1002/jcp.20164.
[12] A. Barlic, M. Drobnic, E. Malicev, N. Kregar-Velikonja, Quantitative analysis of gene expression in human articular chondrocytes assigned for autologous implantation, J. Orthop. Res. Off. Publ. Orthop. Res. Soc. 26 (2008) 847–853, doi:10.1002/jor.20559.
[13] F. Dell'Accio, C. De Bari, F.P. Luyten, Microenvironment and phenotypic stability specify tissue formation by human articular cartilage-derived cells in vivo, Exp. Cell Res. 287 (2003) 16–27, doi:10.1016/S0014-4827(03)00036-3.
[14] D.J. Huey, J.C. Hu, K.A. Athanasiou, Unlike bone, cartilage regeneration remains elusive, Science 338 (2012) 917–921, doi:10.1126/science.1222454.
[15] S.A.H. de Vries, M. van Doeselaar, H.J. Kaper, P.K. Sharma, K. Ito, Notochordal cell matrix as a bioactive lubricant for the osteoarthritic joint, Sci. Rep. 8 (2018) 8875, doi:10.1038/s41598-018-27130-9.
[16] S. Müller, L. Acevedo, X. Wang, M.Z. Karim, A. Matta, A. Mehrkens, S. Schaeren, S. Feliciano, M. Jakob, I. Martin, A. Barbero, W.M. Erwin, Notochordal cell conditioned medium (NCCM) regenerates end-stage human osteoarthritic articular chondrocytes and promotes a healthy phenotype, Arthritis Res. Ther. 18 (2016) 125, doi:10.1186/s13075-016-1026-x.
[17] S.A.H. de Vries, E. Potier, M. van Doeselaar, B.P. Meij, M.A. Tryfonidou, K. Ito, Conditioned medium derived from notochordal cell-rich nucleus pulposus tissue stimulates matrix production by canine nucleus pulposus cells and bone marrow-derived stromal cells, Tissue Eng. Part A. 21 (2015) 1077–1084, doi:10.1089/ten.TEA.2014.0309.
[18] B. Gantenbein, E. Calandriello, K. Wuertz-Kozak, L.M. Benneker, M.J.B. Keel, S.C.W. Chan, Activation of intervertebral disc cells by co-culture with notochordal cells, conditioned medium and hypoxia, BMC Musculoskelet. Disord. 15 (2014) 422, doi:10.1186/1471-2474-15-422.
[19] C.L. Korecki, J.M. Taboas, R.S. Tuan, J.C. Iatridis, Notochordal cell conditioned medium stimulates mesenchymal stem cell differentiation toward a young nucleus pulposus phenotype, Stem Cell Res. Ther. 1 (2010) 18, doi:10.1186/scrt18.
[20] D. Purmessur, R.M. Schek, R.D. Abbott, B.A. Ballif, K.E. Godburn, J.C. Iatridis, Notochordal conditioned media from tissue increases proteoglycan accumulation and promotes a healthy nucleus pulposus phenotype in human mesenchymal stem cells, Arthritis Res. Ther. 13 (2011) R81, doi:10.1186/ar3344.
[21] C.A. Poole, S. Ayad, J.R. Schofield, Chondrons from articular cartilage: I. Immunolocalization of type VI collagen in the pericellular capsule of isolated canine tibial chondrons, J. Cell Sci. 90 (1988) 635–643 (Pt 4).
[22] R.E. Wilusz, J. Sanchez-Adams, F. Guilak, The structure and function of the pericellular matrix of articular cartilage, Matrix Biol 39 (2014) 25–32, doi:10.1016/j.matbio.2014.08.009.
[23] N.A. Zelenski, H.A. Leddy, J. Sanchez-Adams, J. Zhang, P. Bonaldo, W. Liedtke, F. Guilak, Type VI Collagen Regulates Pericellular Matrix Properties, Chondrocyte Swelling, and Mechanotransduction in Mouse Articular Cartilage, Arthritis Rheumatol. (Hoboken, N.J.) 67 (2015) 1286–1294, doi:10.1002/art.39034.
[24] T. Scholzen, J. Gerdes, The Ki-67 protein: from the known and the unknown, J. Cell. Physiol. 182 (2000) 311–322 10.1002/(SICI)1097-4652(200003)182:3<311::AID--JCP1>3.0.CO;2-9.
[25] H.-P. Lee, L. Gu, D.J. Mooney, M.E. Levenston, O. Chaudhuri, Mechanical confinement regulates cartilage matrix formation by chondrocytes, Nat. Mater. 16 (2017) 1243–1251, doi:10.1038/nmat4993.
[26] O. Chaudhuri, L. Gu, D. Klumpers, M. Darnell, S.A. Bencherif, J.C. Weaver, N. Huebsch, H. Lee, E. Lippens, G.N. Duda, D.J. Mooney, Hydrogels with tunable stress relaxation regulate stem cell fate and activity, Nat. Mater. 15 (2016) 326–334, doi:10.1038/nmat4489.
[27] S.A. Jelinsky, J. Archambault, L. Li, H. Seeherman, Tendon-selective genes identified from rat and human musculoskeletal tissues, J Orthop Res 28 (2010) 289–297.
[28] Z. Yang, J.-P. Li, H. Guan, Preparation and characterization of oligomannuronates from alginate degraded by hydrogen peroxide, Carbohydr. Polym. 58 (2004) 115–121, doi:10.1016/j.carbpol.2004.04.022.
[29] F. Wolf, C. Candrian, D. Wendt, J. Farhadi, M. Heberer, I. Martin, A. Barbero, Cartilage tissue engineering using pre-aggregated human articular chondrocytes, Eur. Cell. Mater. 16 (2008) 92–99.
[30] L. De Moor, E. Beyls, H. Declercq, Scaffold Free Microtissue Formation for Enhanced Cartilage Repair, Ann. Biomed. Eng. 48 (2020) 298–311, doi:10.1007/s10439-019-02348-4.
[31] J.H. Jeon, B.G. Yun, M.J. Lim, S.J. Kim, M.H. Lim, J.Y. Lim, S.H. Park, S.W. Kim, Rapid cartilage regeneration of spheroids composed of human nasal septum-derived chondrocyte in rat osteochondral defect model, Tissue Eng. Regen. Med. 17 (2020) 81–90, doi:10.1007/s13770-019-00231-w.
[32] L.S. Moreira Teixeira, J.C.H. Leijten, J. Sobral, R. Jin, A.A. van Apeldoorn, J. Feijen, C. van Blitterswijk, P.J. Dijkstra, M. Karperien, High throughput generated micro-aggregates of chondrocytes stimulate cartilage formation in vitro and in vivo, Eur. Cell. Mater. 23 (2012) 387–399.
[33] J.I. Lee, M. Sato, H.W. Kim, J. Mochida, Transplantatation of scaffold-free spheroids composed of synovium-derived cells and chondrocytes for the treatment of cartilage defects of the knee, Eur. Cell. Mater. 22 (2011) 275–290 discussion 290, doi:10.22203/ecm.v022a21.
[34] M.M.J. Caron, P.J. Emans, M.M.E. Coolsen, L. Voss, D.A.M. Surtel, A. Cremers, L.W. van Rhijn, T.J.M. Welting, Redifferentiation of dedifferentiated human articular chondrocytes: comparison of 2D and 3D cultures, Osteoarthr. Cartil. 20 (2012) 1170–1178, doi:10.1016/j.joca.2012.06.016.
[35] V. Velasco, S.A. Shariati, R. Esfandyarpour, Microtechnology-based methods for organoid models, Microsystems Nanoeng. 6 (2020) 76. https://doi.org/10.1038/s41378-020-00185-3.
[36] R.A. Vertrees, M. McCarthy, T. Solley, V.L. Popov, J. Roaten, M. Pauley, X. Wen, T.J. Goodwin, Development of a three-dimensional model of lung cancer using cultured transformed lung cells, Cancer Biol. Ther. 8 (2009) 356–365, doi:10.4161/cbt.8.4.7432.
[37] A. Przepiorski, V. Sander, T. Tran, J.A. Hollywood, B. Sorrenson, J.-H. Shih, E.J. Wolvetang, A.P. McMahon, T.M. Holm, A.J. Davidson, A Simple Bioreactor-Based Method to Generate Kidney Organoids from Pluripotent Stem Cells, Stem Cell Reports 11 (2018) 470–484, doi:10.1016/j.stemcr.2018.06.018.
[38] F. Mwale, K. Masuda, M.P. Grant, L.M. Epure, K. Kato, S. Miyazaki, K. Cheng, J. Yamada, W.C. Bae, C. Muehleman, P.J. Roughley, J. Antoniou, Short Link N promotes disc repair in a rabbit model of disc degeneration, Arthritis Res. Ther. 20 (2018) 201, doi:10.1186/s13075-018-1625-9.
[39] X. Liu, D. Krishnamoorthy, L. Lin, P. Xue, F. Zhang, L. Chi, R.J. Linhardt, J.C. Iatridis, A method for characterising human intervertebral disc glycosaminoglycan disaccharides using liquid chromatography-mass spectrometry with multiple reaction monitoring, Eur. Cell. Mater. 35 (2018) 117–131, doi:10.22203/eCM.v035a09.
[40] H. He, Q. He, F. Xu, Y. Zhou, Z. Ye, W.-S. Tan, Dynamic formation of cellular aggregates of chondrocytes and mesenchymal stem cells in spinner flask, Cell Prolif 52 (2019) e12587, doi:10.1111/cpr.12587.
[41] K. Schneeberger, N. Sánchez-Romero, S. Ye, F.G. van Steenbeek, L.A. Oosterhoff, I. Pla Palacin, C. Chen, M.E. van Wolferen, G. van Tienderen, R. Lieshout, H. Colemonts-Vroninks, I. Schene, R. Hoekstra, M.M.A. Verstegen, L.J.W. van der Laan, L.C. Penning, S.A. Fuchs, H. Clevers, J. De Kock, P.M. Baptista, B. Spee, Large-Scale Production of LGR5-Positive Bipotential Human Liver Stem Cells, Hepatology 72 (2020) 257–270, doi:10.1002/hep.31037.
[42] A.O. Oseni, P.E. Butler, A.M. Seifalian, Optimization of chondrocyte isolation and characterization for large-scale cartilage tissue engineering, J. Surg. Res. 181 (2013) 41–48, doi:10.1016/j.jss.2012.05.087.
[43] K. Yonenaga, S. Nishizawa, T. Nakagawa, Y. Fujihara, Y. Asawa, A. Hikita, T. Takato, K. Hoshi, Optimal conditions of collagenase treatment for isolation of articular chondrocytes from aged human tissues, Regen. Ther. 6 (2017) 9–14, doi:10.1016/j.reth.2016.08.001.
[44] Z. Lin, J.B. Fitzgerald, J. Xu, C. Willers, D. Wood, A.J. Grodzinsky, M.H. Zheng, Gene expression profiles of human chondrocytes during passaged monolayer cultivation, J. Orthop. Res. Off. Publ. Orthop. Res. Soc. 26 (2008) 1230–1237, doi:10.1002/jor.20523.
[45] N. Ahmed, J. Iu, C.E. Brown, D.W. Taylor, R.A. Kandel, Serum- and growth-factor-free three-dimensional culture system supports cartilage tissue formation by promoting collagen synthesis via Sox9-Col2a1 interaction, Tissue Eng. Part A. 20 (2014) 2224–2233, doi:10.1089/ten.TEA.2013.0559.
[46] J.M. Melero-Martin, M. Al-Rubeai, In Vitro Expansion of Chondrocytes, in: N. Ashammakhi, R.L. Reis, E. Chielline (Eds.), Top. Tissue Eng. Vol. 3, 2007: pp. 1–37.
[47] C. Yu, A. Kornmuller, C. Brown, T. Hoare, L.E. Flynn, Decellularized adipose tissue microcarriers as a dynamic culture platform for human adipose-derived stem/stromal cell expansion, Biomaterials 120 (2017) 66–80, doi:10.1016/j.biomaterials.2016.12.017.
[48] Y.M. Lin, J.F.Y. Lim, J. Lee, M. Choolani, J.K.Y. Chan, S. Reuveny, S.K.W. Oh, Expansion in microcarrier-spinner cultures improves the chondrogenic potential of human early mesenchymal stromal cells, Cytotherapy 18 (2016) 740–753, doi:10.1016/j.jcyt.2016.03.293.
[49] H.H. Yoon, S.H. Bhang, J.-Y. Shin, J. Shin, B.-S. Kim, Enhanced Cartilage Formation via Three-Dimensional Cell Engineering of Human Adipose-Derived Stem Cells, Tissue Eng. Part A. 18 (2012) 1949–1956, doi:10.1089/ten.tea.2011.0647.
[50] J.M. Melero-Martin, M.-A. Dowling, M. Smith, M. Al-Rubeai, Expansion of chondroprogenitor cells on macroporous microcarriers as an alternative to conventional monolayer systems, Biomaterials 27 (2006) 2970–2979, doi:10.1016/j.biomaterials.2006.01.023.
[51] C.A. Tee, Z. Yang, L. Yin, Y. Wu, J. Han, E.H. Lee, Improved zonal chondrocyte production protocol integrating size-based inertial spiral microchannel separation and dynamic microcarrier culture for clinical application, Biomaterials 220 (2019) 119409, doi:10.1016/j.biomaterials.2019.119409.
[52] B. Koh, N. Sulaiman, M.B. Fauzi, J.X. Law, M.H. Ng, R.B.H. Idrus, M.D. Yazid, Three dimensional microcarrier system in mesenchymal stem cell culture: a systematic review, Cell Biosci 10 (2020) 75, doi:10.1186/s13578-020-00438-8.
[53] J. Malda, C.A. van Blitterswijk, M. Grojec, D.E. Martens, J. Tramper, J. Riesle, Expansion of Bovine Chondrocytes on Microcarriers Enhances Redifferentiation, Tissue Eng 9 (2003) 939–948, doi:10.1089/107632703322495583.
[54] M. Akmal, A. Anand, B. Anand, M. Wiseman, A.E. Goodship, G. Bentley, The culture of articular chondrocytes in hydrogel constructs within a bioreactor enhances cell proliferation and matrix synthesis, J. Bone Joint Surg. Br. 88 (2006) 544–553, doi:10.1302/0301-620X.88B4.16498.
[55] P. Gupta, M.-Z. Ismadi, P.J. Verma, A. Fouras, S. Jadhav, J. Bellare, K. Hourigan, Optimization of agitation speed in spinner flask for microcarrier structural integrity and expansion of induced pluripotent stem cells, Cytotechnology 68 (2016) 45–59, doi:10.1007/s10616-014-9750-z.

[56] N. Jounai, K. Kobiyama, F. Takeshita, K.J. Ishii, Recognition of damage-associated molecular patterns related to nucleic acids during inflammation and vaccination, Front. Cell. Infect. Microbiol. 2 (2013) 168, doi:10.3389/fcimb.2012.00168.
[57] J. Yang, Y.S. Zhang, K. Yue, A. Khademhosseini, Cell-laden hydrogels for osteochondral and cartilage tissue engineering, Acta Biomater 57 (2017) 1–25, doi:10.1016/j.actbio.2017.01.036.
[58] E. Schuh, S. Hofmann, K.S. Stok, H. Notbohm, R. Müller, N. Rotter, The influence of matrix elasticity on chondrocyte behavior in 3D, J. Tissue Eng. Regen. Med. 6 (2012) e31–e42, doi:10.1002/term.501.
[59] B. Bachmann, S. Spitz, B. Schädl, A.H. Teuschl, H. Redl, S. Nürnberger, P. Ertl, Stiffness Matters: fine-Tuned Hydrogel Elasticity Alters Chondrogenic Redifferentiation, Front. Bioeng. Biotechnol. 8 (2020) 373, doi:10.3389/fbioe.2020.00373.
[60] H. Park, X. Guo, J.S. Temenoff, Y. Tabata, A.I. Caplan, F.K. Kasper, A.G. Mikos, Effect of swelling ratio of injectable hydrogel composites on chondrogenic differentiation of encapsulated rabbit marrow mesenchymal stem cells in vitro, Biomacromolecules 10 (2009) 541–546, doi:10.1021/bm801197m.
[61] M. Dadsetan, M. Pumberger, M.E. Casper, K. Shogren, M. Giuliani, T. Ruesink, T.E. Hefferan, B.L. Currier, M.J. Yaszemski, The effects of fixed electrical charge on chondrocyte behavior, Acta Biomater 7 (2011) 2080–2090, doi:10.1016/j.actbio.2011.01.012.
[62] S. Nakamura, M. Ikebuchi, S. Saeki, D. Furukawa, K. Orita, N. Niimi, Y. Tsukahara, H. Nakamura, Changes in viscoelastic properties of articular cartilage in early stage of osteoarthritis, as determined by optical coherence tomography-based strain rate tomography, BMC Musculoskelet. Disord. 20 (2019) 417, doi:10.1186/s12891-019-2789-4.
[63] J. Desrochers, M.W. Amrein, J.R. Matyas, Viscoelasticity of the articular cartilage surface in early osteoarthritis, Osteoarthr. Cartil. 20 (2012) 413–421, doi:10.1016/j.joca.2012.01.011.
[64] Q.Y. Zhang, X.H. Wang, X.C. Wei, W.Y. Chen, Characterization of viscoelastic properties of normal and osteoarthritic chondrocytes in experimental rabbit model, Osteoarthr. Cartil. 16 (2008) 837–840, doi:10.1016/j.joca.2007.09.016.
[65] S. Li, L.R. Nih, H. Bachman, P. Fei, Y. Li, E. Nam, R. Dimatteo, S.T. Carmichael, T.H. Barker, T. Segura, Hydrogels with precisely controlled integrin activation dictate vascular patterning and permeability, Nat Mater 16 (2017) 953–961 http://dx.doi.org/10.1038/nmat4954.
[66] S. Nam, J. Lee, D.G. Brownfield, O. Chaudhuri, Viscoplasticity Enables Mechanical Remodeling of Matrix by Cells, Biophys. J. 111 (2016) 2296–2308, doi:10.1016/j.bpj.2016.10.002.
[67] A.R. Brunelle, C.B. Horner, K. Low, G. Ico, J. Nam, Electrospun thermosensitive hydrogel scaffold for enhanced chondrogenesis of human mesenchymal stem cells, Acta Biomater 66 (2018) 166–176, doi:10.1016/j.actbio.2017.11.020.
[68] Y. Tan, H. Huang, D.C. Ayers, J. Song, Modulating Viscoelasticity, Stiffness, and Degradation of Synthetic Cellular Niches via Stoichiometric Tuning of Covalent versus Dynamic Noncovalent Cross-Linking, ACS Cent. Sci. 4 (2018) 971–981, doi:10.1021/acscentsci.8b00170.
[69] X. Zhao, N. Huebsch, D.J. Mooney, Z. Suo, Stress-relaxation behavior in gels with ionic and covalent crosslinks, J. Appl. Phys. 107 (2010) 63509, doi:10.1063/1.3343265.
[70] H.M. Ismail, K. Yamamoto, T.L. Vincent, H. Nagase, L. Troeberg, J. Saklatvala, Interleukin-1 Acts via the JNK-2 Signaling Pathway to Induce Aggrecan Degradation by Human Chondrocytes., Arthritis Rheumatol. (Hoboken, N.J.) 67 (2015) 1826–1836, doi:10.1002/art.39099.
[71] F. Rousset, F. Hazane-Puch, C. Pinosa, M.V.C. Nguyen, L. Grange, A. Soldini, B. Rubens-Duval, C. Dupuy, F. Morel, B. Lardy, IL-1beta mediates MMP secretion and IL-1beta neosynthesis via upregulation of p22phox and NOX4 activity in human articular chondrocytes, Osteoarthr. Cartil. 23 (2015) 1972–1980, doi:10.1016/j.joca.2015.02.167.
[72] G.P. Raeber, M.P. Lutolf, J.A. Hubbell, Molecularly Engineered PEG Hydrogels: a Novel Model System for Proteolytically Mediated Cell Migration, Biophys. J. 89 (2005) 1374–1388, doi:10.1529/biophysj.104.050682.
[73] D.K. Temple, A.A. Cederlund, B.M. Lawless, R.M. Aspden, D.M. Espino, Viscoelastic properties of human and bovine articular cartilage: a comparison of frequency-dependent trends, BMC Musculoskelet. Disord. 17 (2016) 419, doi:10.1186/s12891-016-1279-1.
[74] L.A.S. Callahan, A.M. Ganios, D.L. McBurney, M.F. Dilisio, S.D. Weiner, W.E.J. Horton, M.L. Becker, ECM production of primary human and bovine chondrocytes in hybrid PEG hydrogels containing type I collagen and hyaluronic acid, Biomacromolecules 13 (2012) 1625–1631, doi:10.1021/bm3003336.
[75] L. Duan, B. Ma, Y. Liang, J. Chen, W. Zhu, M. Li, D. Wang, Cytokine networking of chondrocyte dedifferentiation in vitro and its implications for cell-based cartilage therapy, Am. J. Transl. Res. 7 (2015) 194–208.
[76] P.D. Benya, S.R. Padilla, M.E. Nimni, Independent regulation of collagen types by chondrocytes during the loss of differentiated function in culture, Cell 15 (1978) 1313–1321, doi:10.1016/0092-8674(78)90056-9.
[77] R. Mayne, M.S. Vail, P.M. Mayne, E.J. Miller, Changes in type of collagen synthesized as clones of chick chondrocytes grow and eventually lose division capacity, Proc. Natl. Acad. Sci. U. S. A. 73 (1976) 1674–1678, doi:10.1073/pnas.73.5.1674.
[78] K. Von der Mark, V. Gauss, H. Von der Mark, P. Müller, Relationship between cell shape and type of collagen synthesised as chondrocytes lose their cartilage phenotype in culture, Nature 267 (1977) 531–532, doi:10.1038/267531a0.
[79] E.G. Baylon, M.E. Levenston, Osmotic Swelling Responses Are Conserved Across Cartilaginous Tissues With Varied Sulfated-Glycosaminoglycan Contents, J. Orthop. Res. 38 (2020) 785–792, doi:10.1002/jor.24521.
[80] A.J. Sophia Fox, A. Bedi, S.A. Rodeo, The basic science of articular cartilage: structure, composition, and function, Sports Health. 1 (2009) 461–468. https://doi.org/10.1177/1941738109350438.